Langmuir
Article

pubs.acs.org/Langmuir

Effect of Humidity on the Interaction of Dimethyl Methylphosphonate (DMMP) Vapor with SiO_2 and Al_2O_3 Surfaces, Studied Using Infrared Attenuated Total Reflection Spectroscopy

V. M. Bermudez*

Naval Research Laboratory, Washington, D.C. 20375-5347, United States

Received August 24, 2010. Revised Manuscript Received October 13, 2010

Infrared attenuated total reflection spectroscopy has been used to study the interaction of DMMP vapor with SiO_2, Al_2O_3, and AlO(OH) vs relative humidity (RH) and DMMP partial pressure (P/P_0). For SiO_2 the growth with increasing RH of ice-like and liquid-like layers is seen in agreement with previous work. H↔D exchange during exposure to H_2O and D_2O indicates that the ice-like layer is more resistant to exchange, consistent with stronger H-bonding than in the liquid-like layer. Exposure of nominally dry SiO_2 to D_2O indicates the existence of adsorbed H_2O that does not exhibit an ice-like spectrum. The ice-like layer appears only at a finite RH. Exposure of SiO_2 to DMMP in the absence of intentionally added H_2O shows the formation of a strongly bound molecular species followed by a liquid-like layer. The strong interaction involves SiO—H···O=P bonds to surface silanols and/or HO—H···O=P bonds to preadsorbed molecular H_2O. At a finite RH the ice-like layer forms on SiO_2 even in the presence of DMMP up to $P/P_0 = 0.30$. DMMP does not appear to penetrate the ice-like layer under these conditions, and the tendency to form a such a layer drives the displacement of DMMP. Amorphous Al_2O_3 and AlO(OH) do not exhibit an ice-like H_2O layer. Both have a higher surface OH content than does SiO_2, which leads to higher coverages of H_2O or DMMP at equivalent RH or P/P_0. At low P/P_0, for which adsorption is dominated by Al—OH···O=P bonding, a-Al_2O_3 interacts with DMMP more strongly than does AlO(OH) as a result of the higher acidity of OH sites on the former. Up to RH = 0.30 and $P/P_0 = 0.30$, DMMP appears to remain bonded to the surface rather than being displaced by H_2O. H_2O appears to have little or no effect on the total amount of DMMP adsorbed on any of these surfaces, up to an RH of 0.30 and a P/P_0 of 0.30. The results have implications for the transport of DMMP and related molecules on oxide surfaces in the environment.

1. Introduction

Under ambient environmental conditions, oxide surfaces are typically covered with a layer of adsorbed molecular H_2O in addition to surface hydroxyl (OH) groups. The transport of organic reagents through this layer and the competition between such species and H_2O for adsorption sites are important in several areas of technology.[1,2] Studying such phenomena, which depend critically on the structure of the H_2O/substrate interface, requires experimental techniques capable of providing bond-specific chemical information under "practical" steady-state conditions. Infrared (IR) attenuated total reflection (ATR) spectroscopy under steady-state conditions has been used previously[3−6] to observe the interaction of H_2O vapor with thin layers of amorphous SiO_2 (a-SiO_2) on Si. These studies reveal a complex structure that depends on relative humidity (RH). The layer in closest proximity to the hydroxylated SiO_2 surface forms hydrogen bonds (H-bonds) to Si−OH groups resulting in an "ice-like" ordered structure with tetrahedrally coordinated H_2O. The outermost layer is "liquid-like", and there is a transition layer between the two. The different layers are recognizable in the structure of the H_2O vibrational spectrum and its variation with RH. The existence of this multilayer, particularly the ice-like layer, has implications in such areas as tribology and biology. In the former, a strongly bound surface layer of H_2O can affect sliding friction. In the latter, such a layer is important in enhancing biocompatibility of materials by inhibiting the adhesion of proteins, which is a driving mechanism for biofouling.

Similar IR studies have been reported for H_2O vapor interacting with the (0001) surface of bulk α-Al_2O_3 using ATR (ref 7) as well as transmission through a "pile of plates" (ref 8). This system has also been investigated by X-ray diffraction,[9] and X-ray photoemission spectroscopy[10] (XPS) and desorption methods[11] have been applied after high exposures to H_2O vapor. Evidence is again found[8,9] for a partial ordering of the H_2O layer in contact with the surface, which is fully O-terminated when exposed to H_2O vapor[9,10] and which exhibits a structure intermediate between those of α-Al_2O_3 and γ-$Al(OH)_3$. However, in one study[7] a partial wetting of the surface, indicating droplet formation, was documented. Wetting of the Al_2O_3 surface may be more complex than that of SiO_2, since recent work[12] suggests that OH groups in this case can actually make the surface hydrophobic. It is noted that several studies of the H_2O/SiO_2 and H_2O/α-Al_2O_3 interfaces have also been done using sum-frequency generation to probe the

*Phone: +1-202-767-6728. FAX: +1-202-767-1165. E-mail: victor.bermudez@nrl.navy.mil.

(1) Minakata, S.; Komatsu, M. *Chem. Rev.* **2009**, *109*, 711.
(2) Ewing, G. E. *J. Phys. Chem. B* **2004**, *108*, 15953. *Chem. Rev.* **2006**, *106*, 1511.
(3) Asay, D. B.; Kim, S. H. *J. Phys. Chem. B* **2005**, *109*, 16760.
(4) Barnette, A. L.; Asay, D. B.; Kim, S. H. *Phys. Chem. Chem. Phys.* **2008**, *10*, 4981.
(5) Asay, D. B.; Barnette, A. L.; Kim, S. H. *J. Phys. Chem. C* **2009**, *113*, 2128.
(6) Anderson, A.; Ashurst, W. R. *Langmuir* **2009**, *25*, 11549.
(7) Thomas, A. C.; Richardson, H. H. *J. Phys. Chem. C* **2008**, *112*, 20033.
(8) Al-Abadleh, H. A.; Grassian, V. H. *Langmuir* **2003**, *19*, 341.
(9) Eng, P. J.; Trainor, T. P.; Brown, G. E., Jr.; Waychunas, G. A.; Newville, M.; Sutton, S. R.; Rivers, M. L. *Science* **2000**, *288*, 1029.
(10) Liu, P.; Kendelewicz, T.; Brown, G. E., Jr.; Nelson, E. J.; Chambers, S. A. *Surf. Sci.* **1998**, *417*, 53.
(11) Elam, J. W.; Nelson, C. E.; Cameron, M. A.; Tolbert, M. A.; George, S. M. *J. Phys. Chem. B* **1998**, *102*, 7008.
(12) Gentleman, M. M.; Ruud, J. A. *Langmuir* **2010**, *26*, 1408.

Report Documentation Page

Form Approved
OMB No. 0704-0188

1. REPORT DATE	2. REPORT TYPE	3. DATES COVERED
13 OCT 2010		**00-00-2010 to 00-00-2010**

4. TITLE AND SUBTITLE	5a. CONTRACT NUMBER
Effect of Humidity on the Interaction of Dimethyl Methylphosphonate (DMMP) Vapor with SiO2 and Al2O3 Surfaces, Studied Using Infrared Attenuated Total Reflection Spectroscopy	5b. GRANT NUMBER
	5c. PROGRAM ELEMENT NUMBER
6. AUTHOR(S)	5d. PROJECT NUMBER
	5e. TASK NUMBER
	5f. WORK UNIT NUMBER
7. PERFORMING ORGANIZATION NAME(S) AND ADDRESS(ES) **Naval Research Laboratory,Washington,DC,20375**	8. PERFORMING ORGANIZATION REPORT NUMBER
9. SPONSORING/MONITORING AGENCY NAME(S) AND ADDRESS(ES)	10. SPONSOR/MONITOR'S ACRONYM(S)
	11. SPONSOR/MONITOR'S REPORT NUMBER(S)

12. DISTRIBUTION/AVAILABILITY STATEMENT
Approved for public release; distribution unlimited

13. SUPPLEMENTARY NOTES

14. ABSTRACT

15. SUBJECT TERMS

16. SECURITY CLASSIFICATION OF:			17. LIMITATION OF ABSTRACT	18. NUMBER OF PAGES	19a. NAME OF RESPONSIBLE PERSON
a. REPORT **unclassified**	b. ABSTRACT **unclassified**	c. THIS PAGE **unclassified**	**Same as Report (SAR)**	**11**	

ν(O−H) stretching modes; however, these have dealt with liquid H_2O and not with the vapor, which is the subject of interest here. One study[13] applied another laser technique, cavity ring-down spectroscopy, to a study of H_2O vibrational modes at the vapor/bulk-a-SiO_2 interface and found evidence for an ordered monolayer similar to that detected in ATR experiments on thin SiO_2 films.

Computational modeling of the interface between H_2O and either SiO_2 or Al_2O_3 has been carried out using molecular dynamics (MD). For SiO_2 there have been numerous studies using either ab initio density functional theory (DFT) or force-field methods, crystalline or amorphous SiO_2 models (with or without surface silanol), liquid- or vapor-phase H_2O, and planar or porous structures. A wide range of temperatures is also encompassed in the various MD studies. Here, we mention only those works[14−21] that are most closely related to the present experiments. These report results at room temperature for hydroxylated surfaces using either an amorphous model or a series of different crystalline quartz surface planes to represent a disordered substrate. The results are generally consistent with experimental data showing a structured layer characterized by strong H-bonding that transitions to a liquid layer with increasing distance from the surface. However, the detailed structure of this layer depends on the coverage and on the relative positions of surface Si−OH groups. The structured layer is confined to within ∼10 Å from the SiO_2 surface, and the diffusion of H_2O within this layer is slower than in bulk liquid H_2O. In contrast to SiO_2 there has been relatively little computational work[22,23] done for high coverages of H_2O on Al_2O_3. The results for α-Al_2O_3 (0001) concur with the experimentally observed[9] high reactivity between H_2O and the OH-free surface and with the resulting restructuring of the surface. At higher coverage molecular H_2O forms H-bonded structures at OH sites resulting from the initial dissociative adsorption on the bare surface. A recent review[24] discusses the properties of various Al_2O_3 surfaces under ambient conditions.

The interface between H_2O vapor and amorphous SiO_2 or Al_2O_3 has also been studied[25,26] in situ using XPS, near-edge X-ray absorption fine-structure (NEXAFS) and work function measurements. The SiO_2 results call into question the existence of the ice-like layer at room temperature. In particular, work-function data[25] show little or no effect due to formation of the initial H_2O layer. However, in the model proposed by Asay et al.[3] the ice-like layer involves no net dipole moment, which is consistent with the absence of a change in work function.

In the present work we are concerned with the interaction between vapors of dimethyl methylphosphonate ($(CH_3O)_2(CH_3)$-P═O, DMMP) and H_2O while in contact with representative oxide surfaces. The oxides of interest, SiO_2 and Al_2O_3, are chosen because of their presence in many forms of soils, minerals, and building materials and because their surface chemistries have similarities with a wide range of other oxides. The form of Al_2O_3 used here is amorphous (a-Al_2O_3) grown as described in section 2.3. The structure of a-Al_2O_3 has recently been studied[27] using nuclear magnetic resonance (NMR) spectroscopy, which shows that most Al atoms are four- or 5-fold coordinated. Thus, the hydroxylated surface is expected to approximate that of hydroxylated γ-Al_2O_3 (ref 28), which also contains four- and 5-fold-coordinated surface Al sites before hydroxylation.

DMMP is important as a simulant for toxic phosphoryl compounds that constitute hazards to the environment and to personnel. The interaction between DMMP and H_2O (either vapor or liquid) has been studied previously using matrix-isolation IR spectroscopy combined with ab initio computational modeling,[29] by molecular mechanics calculations[30] (see also ref 31), by ab initio theory,[32] and by NMR and IR spectroscopies.[33] In the vapor phase[29] an H-bond forms between a single H_2O and the O atom of the P═O group with a bond energy of 7.7 kcal/mol computed at the MP2/6-31$^+$G(d,p) level. At higher H_2O concentrations,[29,30,33] i.e., in aqueous solution, two H_2O molecules bind to the P═O group of a single DMMP. The O atoms of the CH_3O groups are found[29,30] to be largely ineffective in H-bonding to H_2O. Dissolving DMMP in H_2O is found, in ab initio models,[32] to affect the relative stability of different conformers and to lower the barrier to interconversion relative to the vapor phase.

The adsorption of DMMP vapor on a-SiO_2 (refs 34−37) and on OH-terminated organic self-assembled monolayers (SAMs, refs 38−41) has been studied using primarily IR spectroscopy. A similar molecule (DIMP), in which the CH_3O groups of DMMP are replaced with $(CH_3)_2CHO$, has been studied[42] while interacting with OH-terminated SAMs. An ab initio computational study of DMMP/a-SiO_2 has also been reported.[43] The general consensus is that DMMP adsorbs nondissociatively by formation of one or more O—H···O═P bonds, although one study[35] has suggested H-bonding to the methoxy O atoms. Similar experimental studies have been performed for adsorption on various forms of Al_2O_3 (refs 44−47), and an ab initio computational

(13) Aarts, I. M. P.; Pipino, A. C. R.; Hoefnagels, J. P. M.; Kessels, W. M. M.; van de Sanden, M. C. M. *Phys. Rev. Lett.* **2005**, *95*, 166104.
(14) Notman, R.; Walsh, T. R. *Langmuir* **2009**, *25*, 1638.
(15) Argyris, D.; Cole, D. R.; Striolo, A. *J. Phys. Chem. C* **2009**, *113*, 19591. *Langmuir* **2009**, *25*, 8025.
(16) Lopes, P. E. M.; Murashov, V.; Tazi, M.; Demchuk, E.; MacKerell, A. D., Jr. *J. Phys. Chem. B* **2006**, *110*, 2782.
(17) Du, Z.; de Leeuw, N. H. *Dalton Trans.* **2006**, 2623.
(18) Puibasset, J.; Pellenq, R. J.-M. *J. Chem. Phys.* **2003**, *118*, 5613.
(19) Warne, M. R.; Allan, N. L.; Cosgrove, T. *Phys. Chem. Chem. Phys.* **2000**, *2*, 3663.
(20) Chuang, I.-S.; Maciel, G. E. *J. Phys. Chem. B* **1997**, *101*, 3052.
(21) Lee, S. H.; Rossky, P. J. *J. Chem. Phys.* **1994**, *100*, 3334.
(22) Hass, K. C.; Schneider, W. F.; Curioni, A.; Andreoni, W. *J. Phys. Chem. B* **2000**, *104*, 5527.
(23) Thissen, P.; Grundmeier, G.; Wippermann, S.; Schmidt, W. G. *Phys. Rev. B* **2009**, *80*, 245403. Wippermann, S.; Schmidt, W. G.; Thissen, P.; Grundmeier, G. *Phys. Status Solidi C* **2010**, *7*, 137.
(24) Kelber, J. A. *Surf. Sci. Rep.* **2007**, *62*, 271.
(25) Verdaguer, A.; Weis, C.; Oneins, G.; Ketteler, G.; Bluhm, H.; Salmeron, M. *Langmuir* **2007**, *23*, 9699.
(26) Deng, X.; Herranz, T.; Weis, C.; Bluhm, H.; Salmeron, M. *J. Phys. Chem. C* **2008**, *112*, 9668.
(27) Lee, S. K.; Lee, S. B.; Park, S. Y.; Yi, Y. Y.; Ahn, C. W. *Phys. Rev. Lett.* **2009**, *103*, 095501.
(28) Digne, M.; Sautet, P.; Raybaud, P.; Euzen, P.; Toulhoat, H. *J. Catal.* **2002**, *211*, 1. *J. Catal.* **2004**, *226*, 54.
(29) Ault, B. S.; Balboa, A.; Tevault, D.; Hurley, M. *J. Phys. Chem. A* **2004**, *108*, 10094.
(30) Vishnyakov, A.; Neimark, A. V. *J. Phys. Chem. A* **2004**, *108*, 1435.
(31) Sokkalingam, N.; Kamath, G.; Coscione, M.; Potoff, J. J. *J. Phys. Chem. B* **2009**, *113*, 10292.
(32) Florián, J.; Štrajbl, M.; Warshel, A. *J. Am. Chem. Soc.* **1998**, *120*, 7959.
(33) Eaton, G.; Harris, L.; Patel, K.; Symons, M. C. R. *J. Chem. Soc. Faraday Trans.* **1992**, *88*, 3527.
(34) Siu, E. Y.; Andino, J. M. *Nano* **2008**, *3*, 233.
(35) Kanan, S. M.; Tripp, C. P. *Langmuir* **2001**, *17*, 2213.Kanan, S. M.; Tripp, C. P. *Langmuir* **2002**, *18*, 722.
(36) Henderson, M. A.; Jin, T.; White, J. M. *J. Phys. Chem.* **1986**, *90*, 4607.
(37) Ferguson-McPherson, M. K.; Low, E. R.; Esker, A. R.; Morris, J. R. *J. Phys. Chem. B* **2005**, *109*, 18914.
(38) Bertilsson, L.; Potje-Kamloth, K.; Liess, H.-D. *Thin Solid Films* **1996**, *284−285*, 882.
(39) Bertilsson, L.; Engquist, I.; Liedberg, B. *J. Phys. Chem. B* **1997**, *101*, 6021.
(40) Bertilsson, L.; Potje-Kamloth, K.; Liess, H.-D.; Engquist, I.; Liedberg, B. *J. Phys. Chem. B* **1998**, *102*, 1260.
(41) Bertilsson, L.; Potje-Kamloth, K.; Liess, H.-D.; Liedberg, B. *Langmuir* **1999**, *15*, 1128.
(42) Crooks, R. M.; Yang, H. C.; McEllistrem, L. J.; Thomas, R. C.; Ricco, A. J. *Faraday Discuss* **1997**, *107*, 285.
(43) Bermudez, V. M. *J. Phys. Chem. C* **2007**, *111*, 9314.
(44) (a) Mitchell, M. B.; Sheinker, V. N.; Mintz, E. A. *J. Phys. Chem. B* **1997**, *101*, 11192. (b) Sheinker, V. N.; Mitchell, M. B. *Chem. Mater.* **2002**, *14*, 1257.
(45) Aurian-Blajeni, B.; Boucher, M. M. *Langmuir* **1989**, *5*, 170.

study of adsorption on the hydroxylated γ-Al_2O_3 surface has been done.[48] Adsorption in this case is nondissociative at room temperature and occurs by H-bonding between an acidic OH site and the O atom of the P═O; however, decomposition begins at a little above room temperature. Almost all the SiO_2 and Al_2O_3 studies were performed in vacuo on high-surface-area (HSA) powders.

The objective of the present work is to gain insight into how RH affects the adsorption and transport of DMMP (and, by implication, of similar reagents) in the environment. The importance of RH has been noted previously[49] in a study of activated carbon, where adsorption of H_2O was seen to inhibit that of DMMP. A similar inhibition effect has been reported recently[50] for DMMP adsorption on SiO_2 with preadsorbed H_2O. On the other hand, the interaction of DMMP with OH-terminated SAMs has been seen[41] to increase with RH. Based on the above discussion one expects a complex three-way interaction among DMMP, H_2O and surface OH groups, which will also depend on the acid/base character[48,51] of the OH. It is noted, for example, that the computed adsorption energy (ΔE_{ads}) for DMMP on the hydroxylated SiO_2 surface is 20.0 kcal/mol (ref 43), which is only a little greater than that calculated[52] for the most stable configuration of H_2O dimers on such a surface (748 mev/H_2O = 17.4 kcal/mol). This suggests that competition between DMMP and H_2O for adsorption sites may be an important factor.

2. Experimental Details

2.1. ATR Spectroscopy. The basic experimental approach is reviewed elsewhere.[53] Silicon parallelepipeds (termed "ATR prisms") measuring $25 \times 15 \times 1$ mm^3 were obtained from Harrick Scientific (Pleasantville, NY) or from Spectral Systems (Hopewell Junction, NY). These were prepared from float-zone material in order to avoid the strong absorption band at 1106 cm^{-1} due to the bulk oxygen impurity[54] found in Si grown by the Czochralski (silica crucible) method. The prisms were covered on both sides with an oxide layer, sandwiched between two hollow Teflon blocks[55] and the whole assembly squeezed tightly together to form a vapor-tight seal around the edges of the prism. The cell was fitted with Teflon tubes through which vapor flowed over the exposed prism faces.

Spectra were recorded using a Fourier transform infrared (FTIR) spectrometer with a "narrow-band" $Hg_xCd_{1-x}Te$ (MCT-A) detector. No polarizer was used, and the intrinsic polarization of the beam produced by an FTIR spectrometer is typically fairly weak.[56] Usually 2000 scans were averaged at 4 cm^{-1} resolution, and 2- or 4-fold zero filling and triangle apodization were applied to the interferogram before transformation. Data were obtained by ratioing single-beam spectra recorded with and without reagent in the N_2 stream (see following section), from which was obtained $\delta R/R$, the fractional change in reflectance caused by adsorption. No smoothing and, except where noted, no background subtraction were applied to the data. All spectra are divided by the number of internal reflections to give $\delta R/R$ per reflection.

The internal-reflection angle of incidence of $\theta = 60°$, which is well above the critical angle ($\theta_c \approx 17°$ for Si in the mid-IR), was a compromise.[55] This choice of θ gave a total of eleven internal reflections sampling the vapor-prism interface. A smaller θ would give more reflections per unit length of prism and thus higher sensitivity. However, the longer optical path length through the Si would then move the transmission cutoff (due to multiphonon absorption) to higher energy, which would obscure more of the DMMP spectrum. Furthermore, the amplitude of the evanescent electric field decays as $\exp(-z/d_p)$ with distance (z) into the ambient medium,[57] and the penetration depth (d_p) increases with decreasing θ above θ_c, thus increasing the unwanted contribution from vapor-phase absorption. With the present configuration $d_p/\lambda_{IR} \approx 0.056$ and data could be obtained with essentially no contribution from the vapor.

The range covered in this work, ~4000−1000 cm^{-1}, is limited at the low end by the transmission of the Si ATR prism. This range includes a significant part of the mid-IR spectrum of DMMP, and the structure and mode assignments for the liquid[58,59] and vapor phases[60,61] are discussed elsewhere. Features often seen at 1152 and 1206 cm^{-1} are the ν(C−F) stretching modes in Teflon contacting the optically accessible edges of the Si prism. These are strong and, due to small instabilities in the optical system, often do not completely cancel in the ratio. Strong Si multiphonon absorptions also do not completely cancel in all spectra, which leads to baseline artifacts, particularly near 1450 cm^{-1}.

2.2. Reagent Preparation and Handling. Reagent-grade DMMP (Pfaltz and Bauer, 99.5%), D_2O (Aldrich, 99% D), and locally prepared deionized (DI) H_2O were used as received. Typically the total N_2 flow through the IR cell was 100 mL/min and was kept constant during a series of experiments. Part of this flow was pure, dry N_2 obtained from liquid-N_2 boil-off, which passed through a coil of Cu tubing immersed in a constant-temperature bath at 25.0 °C. Another part was N_2 from the same source after passage through a porous glass "bubbler" (or fritted gas-washing bottle) filled with DMMP. A third part of the flow consisted of N_2 through a second bubbler with H_2O or D_2O and was used to adjust the RH, which was checked with a temperature/dew-point/humidity meter (Model 4080; Control Co.; Friendswood, TX). In the following, RH = 1.00 means a relative humidity of 100%. All reagents were purged of dissolved gases prior to use by flushing N_2 through the bubblers at a high flow rate. The partial-pressures (P/P_0, where P_0 is the vapor pressure at 25 °C) and RH values are based on the relative flow rates. For DMMP, P_0 = 0.84 Torr in the absence of H_2O vapor;[62] for H_2O (D_2O), P_0 = 23.8 (20.5) Torr.[63]

Reagent purity could be checked by passing the effluent from the ATR cell through a 10 cm gas cell (with KBr windows) mounted in the spectrometer sample compartment. No evidence of trace impurities was seen in the IR spectrum of the vapor stream exiting the ATR cell. In performing this analysis the spectrum of the DMMP effluent was compared with vapor-phase data for dried and vacuum-distilled DMMP given elsewhere.[60] Recently an analysis of trace impurities in commercially available DMMP has been reported;[64] however, a systematic search for evidence of these species in the present material was not performed here.

In designing the coadsorption experiments, attention must be given to the suppression of DMMP volatility[49,65] by H_2O vapor.

(46) (a) Templeton, M. K.; Weinberg, W. H. *J. Am. Chem. Soc.* **1985**, *107*, 97. (b) *J. Am. Chem. Soc.* **1985**, *107*, 774.
(47) Davies, P. R.; Newton, N. G. *Appl. Surf. Sci.* **2001**, *181*, 296.
(48) Bermudez, V. M. *J. Phys. Chem. C* **2009**, *113*, 1917.
(49) Kaplan, D.; Nir, I.; Shmueli, L. *Carbon* **2006**, *44*, 3247.
(50) Hearn, J.; Weber, R.; Henley, M.; Cory, M.; Runge, K.; Hurley, M.; Taylor, DeC.; Burns, D. **2009** Chemical and Biological Defense Science and Technology Conference (Dallas, TX; Nov. 16−20, 2009), Poster T201.
(51) Leung, K.; Nielsen, I. M. B.; Criscenti, L. J. *J. Am. Chem. Soc.* **2009**, *131*, 18358.
(52) Yang, J.; Meng, S.; Xu, L.; Wang, E. G. *Phys. Rev. B* **2005**, *71*, 035413.
(53) Hind, A. R.; Bhargava, S. K.; McKinnon, A. *Adv. Colloid Interface Sci.* **2001**, *93*, 91.
(54) Kaiser, W.; Keck, P. H.; Lange, C. F. *Phys. Rev.* **1956**, *101*, 1264.
(55) Queeney, K. T.; Fukidome, H.; Chaban, E. E.; Chabal, Y. J. *J. Phys. Chem. B* **2001**, *105*, 3903.
(56) Sperline, R. P. *Appl. Spectrosc.* **1991**, *45*, 677.
(57) Harrick, N. J. *Internal Reflection Spectroscopy*; Harrick Scientific: Ossining, NY, 1987.
(58) van der Veken, B. J.; Herman, M. A. *Phosphorous Sulfur* **1981**, *10*, 357.
(59) Moravie, R. M.; Froment, F.; Corset, J. *Spectrochim. Acta* **1989**, *45A*, 1015.
(60) van der Veken, B. J.; Herman, M. A. *J. Mol. Struct.* **1983**, *96*, 233.
(61) Bermudez, V. M. *J. Phys. Chem. C* **2007**, *111*, 3719.
(62) Butrow, A. B.; Buchanan, J. H.; Tevault, D. E. *J. Chem. Eng. Data* **2009**, *54*, 1876.
(63) Besley, L.; Bottomley, G. A. *J. Chem. Thermodyn.* **1973**, *5*, 397.
(64) Hoggard, J. C.; Wahl, J. H.; Synovec, R. E.; Mong, G. M.; Fraga, C. G. *Anal. Chem.* **2010**, *82*, 689.
(65) Tevault, D. E.; Buchanan, J. H.; Buettner, L. C. *Int. J. Thermophys.* **2006**, *27*, 486.

Data reported by Tevault et al.[65] show the maximum DMMP partial pressure that can be sustained for a given temperature and RH. Attempting to increase P/P_0 beyond this point leads to precipitation in the form of an aerosol.[49] Thus, for example, at 25 °C and RH = 0.33 the maximum P/P_0 for DMMP is about 0.41. The dew point for such a mixture[65] is ~25.0 °C. In the present work, the semitransparent Teflon tubing downstream from the region of mixing was checked for any indication of aerosol formation. This was done by illuminating with a bright light and looking for evidence of light scattering.[49]

2.3. Sample Preparation and Characterization. Following previous[3−5] work, the *a*-SiO_2/Si samples were grown using ultraviolet/ozone (UV/O_3) oxidation. This was done in order to facilitate comparison with these studies. Some of the data reported in ref 6, with which the present results will also be compared, were obtained for *a*-SiO_2 films grown by plasma oxidation. Data for a thin thermal oxide were also obtained in the course of the present work in order to check for any dependence of the results on oxide growth method. The ATR prism was first cleaned by immersion in warm (50 °C) acetone for ~1 h and then subjected to UV/O_3 oxidation for 1 h at nominally 300 °C (Model UV-1; Samco International; Kyoto, Japan). The feed-gas was O_2 enriched in O_3 by passage through a "silent discharge" prior to entering the UV-irradiated area. The UV radiation, which produces additional O_3, was provided by a low-pressure Hg-vapor/inert-gas lamp emitting mainly at λ_{UV} = 254 nm. The oxide was then stripped in aqueous HF solution and the sample rinsed in DI H_2O and dried in a stream of N_2. The UV/O_3 treatment was repeated for 1 h, followed by a 15-min immersion in "RCA-1" solution (H_2O:NH_4OH (30%):H_2O_2 (30%) in a 3:1:1 ratio by volume) at 75−80 °C, followed by rinsing in DI H_2O and drying in N_2.

The contact angle (CA) for DI H_2O was measured at several spots on the clean oxidized surface. The CA was always < 10° and often < 5°, which indicates a highly hydrophilic surface, i.e., one which is both free of significant hydrocarbon contamination and high in silanol coverage.[66] Previous work[67,68] for UV/O_3 oxidation of Si indicates a limiting SiO_2 thickness of about 2.5 nm for irradiation in pure O_2 (some of which is photochemically converted to O_3) at a substrate temperature of 300 °C. The present samples were analyzed using XPS, which showed an SiO_2 thickness of ~2.1 nm. Survey XPS scans were also done to check for contamination, and the samples were further characterized by IR transmission (see the Supporting Information). Films of *a*-SiO_2 were also prepared by thermal oxidation in dry O_2 at 800 °C. Prior to growth the substrate was cleaned in acetone and in RCA-1 solution as described above. The oxide thickness, determined from XPS measurements, was ~8.1 nm. Thermal oxides of thickness ≥3 nm are essentially equivalent to bulk *a*-SiO_2, as shown by IR spectroscopy.[69] The CA results after RCA-1 cleaning were the same as those described above for the UV/O_3 oxide. The oxidized sample was cleaned again in RCA-1 solution before mounting in the ATR cell.

Amorphous Al_2O_3 films were prepared commercially by radio frequency magnetron sputter deposition (PVD Products; Wilmington, MA) onto Si ATR prisms. The film thickness was ~8.5 nm, which has been shown[70] to be sufficient to achieve IR optical properties equivalent to those of bulk material. The samples were cleaned by immersion in warm (~50 °C) hexane and warm acetone for 10 min each followed by a 30-min UV/O_3 exposure at nominal room temperature. The H_2O CA was not measured since contact with liquid H_2O is known to alter the surface properties of Al_2O_3 (discussed in section 3.1.4 below). After mounting in the ATR cell, the sample was exposed overnight to a 100 mL/min flow of N_2 saturated with H_2O (RH = 1.0) in order to hydroxylate the surface and to preclude any significant change in the surface condition during subsequent experiments involving H_2O vapor. The characterization of the *a*-Al_2O_3 samples using XPS and IR transmission is described in the Supporting Information.

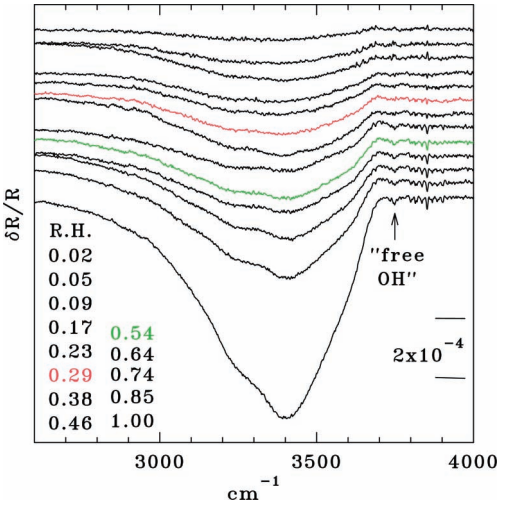

Figure 1. IR ATR data for the ν(O−H) stretching band of H_2O adsorbed on UV/O_3 SiO_2 vs RH at room temperature (24 °C). The vertical scale gives $\delta R/R$ per internal reflection. The numbers give the RH for each spectrum starting with the upper-most, where RH = 1.00 means a relative humidity of 100%. The spectra have been displaced vertically for clarity, but the small sloping background present in some spectra has not been removed. Two of the spectra are shown in color to help guide the eye. The weak feature labeled "free OH" is discussed in section 3.1.1.

3. Results and Discussion

3.1. Amorphous SiO_2. The discussion will begin with an examination of the pure-H_2O and pure-DMMP steady-state IR ATR data which is necessary for an appreciation of the coadsorption results. The H_2O data will also serve to validate the present samples and methods by comparison with previous results. Infrared data for DMMP at high P/P_0 have not, to our knowledge, been reported previously for SiO_2 or Al_2O_3.

3.1.1. H_2O in Pure N_2. Figure 1 shows data for SiO_2 vs RH (in the absence of DMMP). The results essentially reproduce those given previously,[3−6] which reveal a band at about 3240 cm^{-1} due to the ice-like layer and another at about 3400 cm^{-1} assigned to the liquid-like layer. In contrast, the δ(HOH) bending mode at 1640 cm^{-1} (not shown) does not indicate any distinction between the ice- and liquid-like phases.[3−6] The weak, sharp structure in the 3600−3900 cm^{-1} range is due to H_2O vapor. In the lower-RH spectra this arises from the incomplete dry-N_2 purging of the optical path. At higher RH it represents the contribution from H_2O vapor in the cell under steady-state conditions. The low intensity relative to that of the surface species indicates the excellent rejection of vapor contributions in the present ATR experiment. A weak feature at ~3740 cm^{-1}, labeled "free OH", is seen in most IR data for thin H_2O films and is assigned to dangling (i.e., not H-bonded) O−H bonds on the surface of the H_2O layer. Figure 2 shows the isotherm, derived from the data in Figure 1, which is similar to that of Asay et al.[3] This isotherm, and those reported later for other materials, are of

(66) Cras, J. J.; Rowe-Taitt, C. A.; Nivens, D. A.; Ligler, F. S. *Biosens. Bioelectron.* **1999**, *14*, 683.
(67) Ishikawa, Y.; Shibamoto, T.; Nakamichi, I. *Jpn. J. Appl. Phys.* **1992**, *31*, 1148.
(68) Saitoh, T.; Kobayashi, D.; Kimura, D.; Asai, K. *Mater. Res. Soc. Symp. Proc.* **1999**, *569*, 101.
(69) Queeney, K. T.; Weldon, M. K.; Chang, J. P.; Chabal, Y. J.; Gurevich, A. B.; Sapjeta, J.; Opila, R. L. *J. Appl. Phys.* **2000**, *87*, 1322.
(70) Brüesch, P.; Kötz, R.; Neff, H.; Pietronero, L. *Phys. Rev. B* **1984**, *29*, 4691.

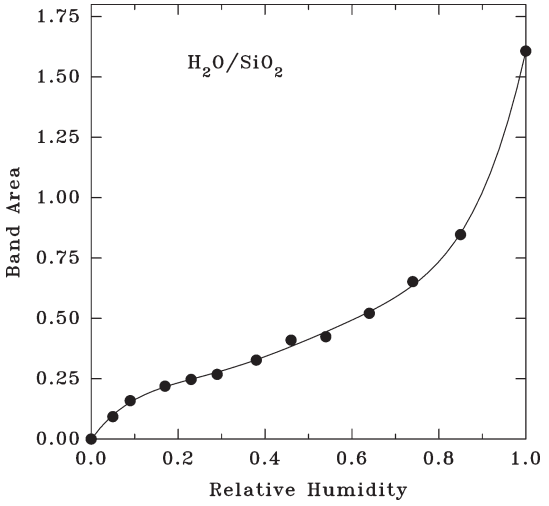

Figure 2. Adsorption isotherm constructed by plotting the integrated band area in Figure 1 vs RH. The smooth curve through the points is simply a visual aid. The vertical scale is in units of total absorbance (not divided by the number of internal reflections) times wavenumbers and is given explicitly in order to facilitate quantitative comparison with isotherms for other materials.

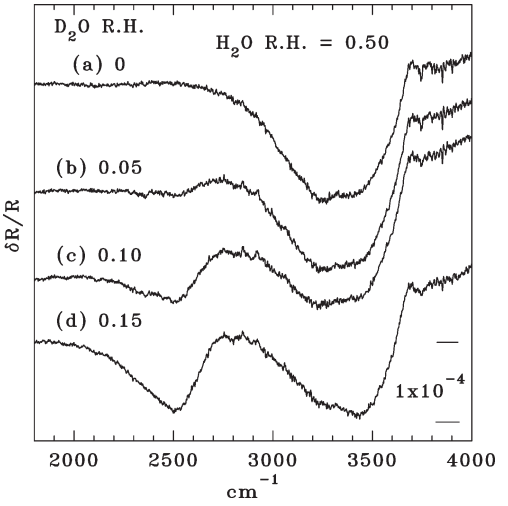

Figure 3. Data for exposure of SiO_2 to mixed H_2O and D_2O. The H_2O was maintained at RH = 0.50 while the RH of D_2O was increased in stages. The sloping background present in some spectra has not been removed. Assuming complete isotopic mixing, the H_2O:HDO:D_2O relative concentrations are (a) 1:0:0, (b) 0.83:0.16:0.01, (c) 0.69:0.28:0.03, and (d) 0.59:0.36:0.05.

the type II form[71] characteristic of a hydrophilic surface, one for which the heat of H_2O adsorption is greater than that of condensation.

There are, however, some differences from previous results. Asay et al.,[3,5] working with a sample at slightly below room temperature, observed the sequential formation of ice-like, mixed (ice-like and liquid-like), and liquid-like phases with increasing RH. At 20.8 °C and RH < 0.30, the spectrum was dominated by the ice-like phase. On the other hand, Anderson and Ashurst[6] observed the simultaneous presence of both forms at all values of RH, with the ice-like band always being the more intense. The results in Figure 1 exhibit characteristics of both sets of data. Even at the lowest RH the spectrum appears to be a sum of approximately equal contributions from both forms; however, the liquid-like layer becomes dominant at higher RH values.

It is possible to propose a tentative interpretation for these differences. The results of Asay et al.[3,5] suggest a uniform growth of an ice-like layer at low RH, followed by growth of a liquid-like multilayer at higher RH. Those of Anderson and Ashurst,[6] on the other hand, are consistent with the formation of droplets that increase in size toward higher RH but which never coalesce into a continuous layer. The present results seem to indicate the initial formation of droplets that, with increasing RH, merge into a continuous multilayer. These differences probably arise from variations in the SiO_2 preparation and/or surface condition. Here "surface condition" refers to the coverage and identity (e.g., isolated vs geminal) of Si−OH groups as well as to the coverage of adsorbed H_2O remaining after purging in dry N_2 at room temperature. It is well established[72−75] that evacuation at an elevated temperature is needed to remove all H_2O which is H-bonded to the SiO_2 surface. Hence, any layer growth under the present conditions occurs in addition to a preadsorbed H_2O layer, further evidence for which will be given in the following section.

Figure 3 shows data for SiO_2 in H_2O vapor at an RH of 0.50 and an increasing RH of D_2O. An RH of 0.50 is sufficient for completion of the H_2O ice-like layer (cf. Figure 1). The IR spectrum of isotopically mixed water is complex and is discussed in detail elsewhere, most recently in ref 76. In Figure 3, addition of D_2O leads to the gradual attenuation of the H_2O ice-like band at ~3240 cm^{-1}. The loss of ice-like intensity is interpreted as the result of disordering caused by the admixing of HDO and D_2O. For higher RHs of D_2O, interpretation is difficult due to the fact that the spectra involve relatively large contributions from HDO, for which ν(O−H) and ν(O−D) differ only slightly from those of H_2O and D_2O (ref 77). The formation of HDO is revealed by the appearance of the δ(HOD) bending mode[77] at 1450 cm^{-1} (not shown). It is noteworthy, however, that the H_2O ice-like band remains detectable even for a D_2O/H_2O ratio of ~1/3 and beyond, disappearing completely only for a ratio of ~1/1 (not shown), for which the relative H_2O:HDO:D_2O concentration is 0.25:0.50:0.25. The fact that the ice-like band does eventually disappear indicates that the shoulder at ~3240 cm^{-1} in Figure 3 is not due to ice-like HDO.

These results suggest that isotope exchange involving the ice-like layer is slower than for the liquid-like layer, which is consistent with a stronger intermolecular interaction within the ice-like layer. Some MD work has also found that exchange[17] of H_2O between the two layers is slow and that lateral diffusion[14] within the ice-like layer is slower than in bulk H_2O by a factor of ~2. A further discussion of H_2O/D_2O isotope experiments is given in the following section.

3.1.2. DMMP in Dry N_2. Figure 4 shows results for DMMP over a range of partial pressures in the absence of intentionally added H_2O. The most significant effect is a blue-shift in the P═O stretch (ν(P═O)) with increasing P/P_0. The limiting peak positions vary somewhat from run to run, falling in the 1222−1230 and 1246−1250 cm^{-1} ranges for low and high P/P_0 respectively. This variability could be related to the amount of preadsorbed molecular H_2O (discussed later in this section). The ν(P═O) mode is known[33,41] to be sensitive to the surrounding medium. In the vapor, it occurs at 1276 cm^{-1}; whereas, in the liquid, intermolecular

(71) Morrison, S. R. *The Chemical Physics of Surfaces*; Plenum: New York, 1977; Chapter 7.
(72) McDonald, R. S. *J. Phys. Chem.* **1958**, *62*, 1168.
(73) Zhdanov, S. P.; Kosheleva, L. S.; Titova, T. I. *Langmuir* **1987**, *3*, 960.
(74) Burneau, A.; Barrès, O.; Gallas, J. P.; Lavalley, J. C. *Langmuir* **1990**, *6*, 1364. Gallas, J. P.; Lavalley, J. C.; Burneau, A.; Barrès, O. *Langmuir* **1991**, *7*, 1235.
(75) Feng, A.; McCoy, B. J.; Munir, Z. A.; Cagliostro, D. E. *J. Colloid Interface Sci.* **1996**, *180*, 276.
(76) Riemenschneider, J.; Wulf, A.; Ludwig, R. *Z. Phys. Chem.* **2009**, *223*, 1011.
(77) Maréchal, Y. *J. Chem. Phys.* **1991**, *95*, 5565.

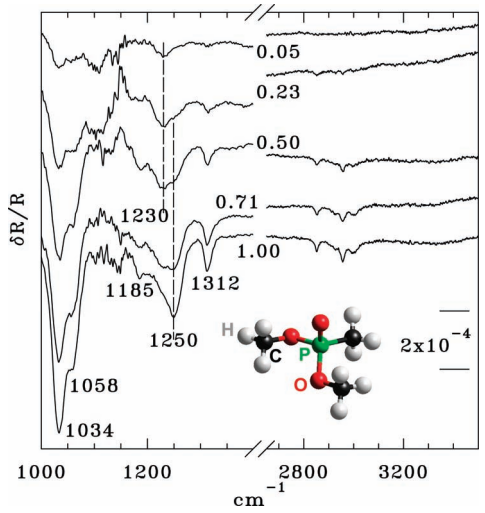

Figure 4. Similar to Figure 1 but for exposure to DMMP vapor at room temperature in the absence of intentionally added H_2O. The numbers 0.05, etc. give P/P_0 for each spectrum. Peak energies are labeled, and the spectra have been displaced vertically for clarity. The noisy, irregular region from about 1100 to 1150 cm^{-1} corresponds to a region of strong multiphonon absorption in the Si ATR prism in which the sample is almost completely opaque. The vertical dashed lines indicate the shift in ν(P═O) with coverage. The inset shows a model for DMMP.

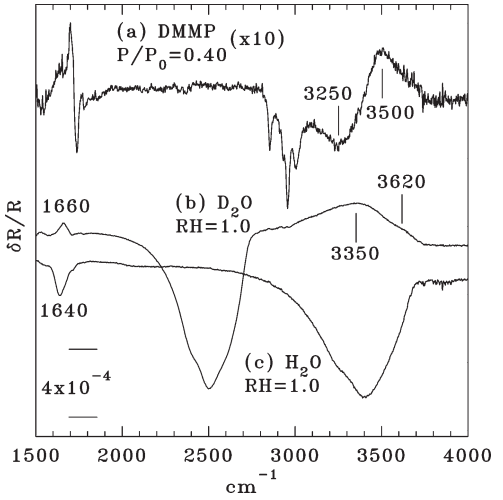

Figure 5. Data showing the effects of adsorption on ν(O−H) modes. (a) DMMP in dry N_2 (P/P_0 = 0.40) after subtraction of a polynomial background (see section 3.1.3). (b) pure D_2O (RH = 1.0). (c) pure H_2O (RH = 1.0). The $\delta R/R$ scale applies to traces (b) and (c). $\delta R/R$ for trace (a) has been expanded by a factor of 10. The δ(HOH) bending mode appears at slightly different energies in (b) and (c), as indicated. The region near 1500 cm^{-1} is affected by a slight miscancellation of the strong Si multiphonon absorption at ~1450 cm^{-1}.

interactions shift it to 1245 cm^{-1} (refs 58−61). In H_2O solution,[33] ν(P═O) is found at 1206 cm^{-1}, and the corresponding mode of a second conformer appears at 1185 cm^{-1}. At low P/P_0 the large red-shift relative to the vapor ($\Delta\nu$(P═O) ≥ −46 cm^{-1}) suggests a strong bonding interaction involving the phosphoryl O atom. At high P/P_0, ν(P═O) is slightly higher than for liquid DMMP but much lower than for the vapor. This indicates that the DMMP is in an environment essentially like that of the pure liquid. Similar shifts with increasing coverage[39] at a sample temperature of 100 K or with increasing P/P_0 at room temperature[40,42] were seen for DMMP and DIMP on OH-terminated SAMs.

Previous studies of DMMP adsorption on other forms of *a*-SiO_2, under vacuum conditions, found $\Delta\nu$(P═O) = −19 (ref 35) and −41 cm^{-1} (ref 37) relative to the vapor phase. In view of the present results, this difference could be related to the DMMP coverage, the extent of surface hydoxylation or the nature of the Si−OH sites (e.g., isolated vs geminal). Computational results[43] indicate that H-bonding between the phosphoryl O atom and two Si−OH groups is the most stable mode of adsorption on *a*-SiO_2. For this structure, $\Delta\nu$(P═O) = −29 cm^{-1} is calculated. Other, less environmentally sensitive modes are the δ_s(P−CH_3) symmetric deformation at 1312 cm^{-1}, the ρ(O−CH_3) rocking mode at 1185 cm^{-1} and the out-of-phase and in-phase ν(P−O−CH_3) stretches at 1034 and 1058 cm^{-1} respectively. None of these show any pronounced shift with changing P/P_0. In particular, the ν(P−O−CH_3) modes appear at the liquid-phase frequencies over the full range of P/P_0 (vs 1050 and 1075 cm^{-1} in the vapor phase). Since the methoxy groups are not directly involved in adsorption this suggests that there is a significant intermolecular interaction involving either DMMP or preadsorbed H_2O.

Figure 5 shows the effects of adsorption on the ν(O−H) spectrum.[72−75] Upward- (downward-) pointing features correspond to species removed (added) by adsorption. The DMMP data (Figure 5a) show the replacement of "moderately-strong" H-bonds[72] (the upward-pointing band at ~3500 cm^{-1}) with stronger Si═OH···O═P bonds giving the downward-pointing band at ~3250 cm^{-1}. Since the two bands overlap, giving a derivative-like structure, the exact positions of the bands being added and removed are difficult to determine. Most of the change in the ν(O−H) spectrum is complete at low DMMP partial pressure ($P/P_0 \leq 0.20$), for which the intensity of the 1230 cm^{-1} ν(P═O) peak (Figure 4) reaches saturation. This suggests that the changes arise from a replacement of Si−OH···OH_2 bonds in favor of Si═OH···O═P bonds. Previous studies of DMMP adsorption on other forms of silica found a broad band at 3223 cm^{-1} (ref 35) or 3380 cm^{-1} (ref 37) for ν(O−H) in an Si−OH bonded to DMMP.

Figure 5b shows the spectrum of OH groups (in the absence of DMMP) that can exchange with D_2O and that are, therefore, chemically accessible. These will now be discussed in the context of preadsorbed H_2O, which is present[72−75] at room temperature and RH = 0. The broad band centered at ~3350 cm^{-1} represents strongly interacting Si−OH groups and adsorbed molecular H_2O. A shoulder is seen at ~3620 cm^{-1}, which can be assigned to Si−OH groups weakly interacting with each other or with H_2O. A second D_2O spectrum, completed about 20 min after the one shown, exhibited only a small (~10%) further increase in the intensity (but no change in the shape) of the OH and D_2O bands. This shows that most of the H ↔ D exchange was complete during the first scan. Following this experiment the cell was thoroughly purged with H_2O vapor to remove residual D. For comparison, Figure 5c shows data for pure H_2O at RH = 1.0.

Note that Figure 5a is shown with the $\delta R/R$ scale expanded 10-fold relative to spectra b and c in Figure 5. The results show that only a small fraction (at most ~10%) of the total surface OH content (Si−OH and H_2O) interacts strongly with DMMP. Results for other forms of silica,[35,37] obtained under conditions of low adsorbed-H_2O coverage, indicate that a much larger fraction of the total OH content is affected by DMMP. The presence of a high coverage of H_2O relative to Si−OH can be seen by examining the δ(HOH) bending mode in the 1600−1700 cm^{-1} range. It is difficult to distinguish Si−OH from H_2O in the ν(O−H) spectrum, whereas the δ(HOH) mode is unique to molecular H_2O. In Figure 5b the δ(HOH)/ν(O−H) ratio of integrated areas (~0.06) is essentially

the same as that of pure H_2O (Figure 5c), indicating that most of the exchangeable OH is in the form of molecular H_2O. These results confirm the existence of a high (relative to Si−OH) coverage of molecular H_2O after prolonged purging in dry N_2 at room temperature.

It is noteworthy that this preadsorbed H_2O layer does not exhibit an ice-like ν(O−H) spectrum since there is no clear indication of a band at ~3240 cm^{-1} (cf. Figure 1). The ice-like structure appears to form only in an ambient with a finite RH. This can be understood if the dominant interaction for preadsorbed H_2O is with Si−OH groups. The ice-like layer, on the other hand, involves a strong intermolecular interaction leading to tetrahedrally coordinated H_2O. Thus, at finite RH, the preadsorbed H_2O may act as a connective- or a transition layer between the hydroxylated SiO_2 surface and the ice-like layer. It is possible that, at finite RH, adsorbed H_2O modifies the preadsorbed layer, in effect incorporating it into the ice-like layer. However, data at low RH (Figure 1) show no evidence of the removal of a band near 3350 cm^{-1}, which suggests that preadsorbed H_2O is not strongly affected by the growth of the ice-like layer.

For H_2O at RH = 1.0 (Figure 5c), δ(HOH) appears at 1640 cm^{-1}, which is characteristic of liquid H_2O; whereas, it occurs at 1660 cm^{-1} for the H_2O remaining after purging the cell with dry N_2 (Figure 5b). This blue-shift indicates a relatively strong H-bonding interaction[78,79] consistent with the resistance of this H_2O to easy desorption. H-bonding shifts ν(O−H) and δ(HOH) in opposite directions, and the energies are known[79] to be correlated in different forms of ice. A ν(O−H) of ~3350 cm^{-1}, as in Figure 5b, correlates with a δ(HOH) of ~1680 cm^{-1}, which is fairly close to the value of 1660 cm^{-1} seen here. In the presence of DMMP, the δ(HOH) region becomes complex. The sharp, derivative-like structure near 1700 cm^{-1} is believed to result from the interaction of DMMP with a small concentration of impurity C═O groups, which evidently does not affect the formation of the ice-like layer. C 1s XPS data (see the Supporting Information) indicate a coverage of ~0.08 monolayers of such species, and a slight blue-shift in the intense ν(C═O) absorption band, as a result of DMMP adsorption, would give the observed derivative-like line shape. This feature appears to be superimposed on an upward-pointing peak at ~1660 cm^{-1} indicating the displacement of adsorbed H_2O.

The conclusion at this point is that, at RH ≈ 0 and P/P_0 < ~0.50, a complex surface phase is formed consisting of DMMP and preadsorbed H_2O strongly interacting with each other and with Si−OH. A similar model has been proposed[41] for DMMP at P/P_0 = 0.02 interacting with OH-terminated SAMs in humid N_2. In the present case, DMMP and H_2O may both H-bond to Si−OH, forming a mixed monolayer, or displaced H_2O may adsorb on top of the DMMP. It is also possible that both processes occur simultaneously. At higher P/P_0 and RH ≈ 0 (Figure 4), a liquid-like DMMP layer forms on top of this initial layer.

3.1.3. DMMP in Wet N_2. Figures 6 and 7 show data for different RHs and DMMP P/P_0 values. These were obtained by mixing separate flows of pure N_2 and of N_2 saturated with either H_2O or DMMP. The maximum RH of 0.30 was selected so as to allow a sufficiently high DMMP P/P_0 for clear observation of the DMMP spectrum without exceeding the dew-point restriction discussed in section 2.2. For reference, traces (a) and (b) in either figure show data for pure H_2O and pure DMMP respectively. Figure 6b also shows, for illustration, the type of background that

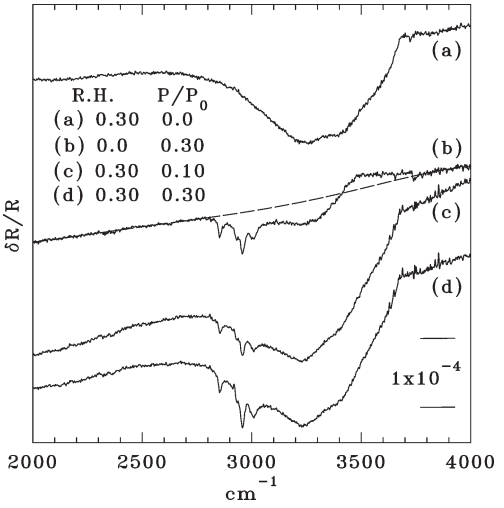

Figure 6. Data in the ν(O−H) and ν(C−H) range for the coadsorption of H_2O and DMMP. RH and P/P_0 give the vapor-phase concentrations of H_2O and DMMP respectively. The spectra have been displaced vertically for clarity. The dashed line in trace (b) illustrates the type of background that was subtracted to produce spectra like that in Figure 5a. This was obtained by fitting a single polynomial to the 2000−2700 and 3800−4000 cm^{-1} regions.

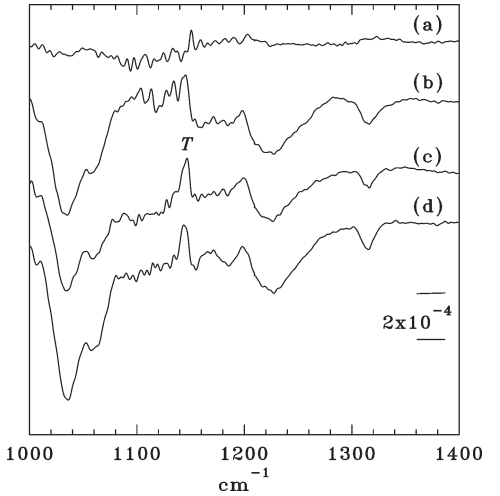

Figure 7. Data in the low-frequency part of the spectrum corresponding to those in Figure 6. The labels correspond to those in Figure 6. The upward-pointing feature labeled ***T*** at ~1145 cm^{-1} is due to miscancellation of a strong Teflon absorption (see section 2.1).

was subtracted to obtain the spectrum shown in Figure 5a. Spectra like those in Figures 6d and 7d were also recorded using D_2O in place of H_2O. There was no sign of H ↔ D exchange involving the CH_3 groups of DMMP, indicating that exchange of H between DMMP and H_2O is not involved under the present conditions.

Two points are noteworthy. First, the presence of H_2O does not appear to have a strong effect on the total amount of adsorbed DMMP, as shown by the comparable DMMP band intensities at P/P_0 = 0.30 with and without added H_2O vapor. Conclusions about adsorbate coverage based on IR data must be qualified by noting that interaction between coadsorbed species can affect intensities. For example, relative intensities differ in the IR spectra of DMMP vapor vs liquid. Furthermore, the FTIR beam is not completely depolarized.[56] Hence, if an adsorbate is not randomly oriented, then reorientation with respect to the surface in response

(78) Paul, S. O.; Ford, T. A. *J. Cryst. Spectrosc. Res.* **1986**, *16*, 811.
(79) Hernandez, J.; Uras, N.; Devlin, J. P. *J. Chem. Phys.* **1998**, *108*, 4525.

to coadsorbed species can also change band intensities. In contrast, H_2O enhances the adsorption of DMMP on OH-terminated SAMs as shown[41] using both IR data and measurements with a surface acoustic wave device, which is sensitive to changes in the total adsorbate mass.

Second, DMMP does not inhibit the formation of an ice-like layer, as shown by the continued clear presence of the ~3240 cm^{-1} band at $P/P_0 = 0.30$. There does appear to be a slight red-shift or broadening of the liquid-like band, probably due to H-bonding to DMMP. Matrix-isolation studies[29] show that in a 1:1 H-bonded complex of H_2O and DMMP, ν(O−H) red-shifts by 203 cm^{-1} relative to the value for H_2O isolated in an Ar matrix (3639 cm^{-1}). However, there is apparently no significant disruption of the ice-like layer. This suggests that, under these conditions, DMMP does not penetrate into or through this layer and that ice-like bonding is sufficiently strong to overcome SiO—H···O=P bonding. For OH-terminated SAMs, in which the OH groups form an H-bonded network, ν(O−H) is found[40] at ~3350 cm^{-1}. Disrupting this network by H-bonding to adsorbed DMMP shifts ν(O−H) to 3450 cm^{-1} suggesting a weaker H-bond to DMMP. In the present ice-like layer the ν(O−H) of ~3240 cm^{-1} indicates stronger H-bonding than for an OH-terminated SAM, one which persists at least up to a DMMP P/P_0 of 0.30. The possibility has been considered that the apparent ice-like band in Figure 6c,d might instead actually result from an interaction between DMMP and H_2O. However, corresponding results (section 3.2) for a-Al_2O_3 and AlO(OH), which show no ice-like layer, also show no band near 3240 cm^{-1} for coadsorbed H_2O and DMMP.

The data in Figures 6 and 7 were recorded in the sequence (b), (c), and (d), i.e., by introducing H_2O vapor into an initially dry flow of DMMP. Data (not shown) recorded in the sequence (a), (c), and (d), by introducing DMMP into a flow of humid N_2, gave essentially the same results. However, unlike in Figure 6, the liquid-like ν(O−H) band remained well-defined as DMMP was added. When DMMP is added to humid N_2 the liquid-on-ice H_2O layer structure is already well-formed before introduction of the DMMP; whereas, in the reverse sequence, H_2O must displace adsorbed DMMP in order to form the ice-like layer.

In the low-frequency range (Figure 7) there is no strong effect on the DMMP spectrum due to addition of H_2O. Under "dry" conditions (Figure 7b) ν(P=O) appears at 1226 cm^{-1} with an asymmetry to higher energy suggesting the onset of the liquid-like DMMP layer. There is little or no change in ν(P=O) as H_2O is added. Bertilsson et al.[41] found ν(P=O) at 1235 cm^{-1} for DMMP bonded to an OH-terminated SAM in the absence of H_2O. With the addition of 4 H_2O per DMMP this mode shifts to about 1226 cm^{-1}, and a further increase in H_2O coverage shifts it to about 1222 cm^{-1}. The present results suggest that DMMP already interacts with preadsorbed H_2O (discussed in section 3.1.2) before the RH is increased by the intentional addition of H_2O.

Taken together, these data suggest mixing of DMMP with the liquid-like H_2O layer, forming in effect an ultrathin aqueous solution on top of an intact ice-like layer. The strong H-bonding within the ice-like layer apparently makes it resistant to disruption by DMMP and, furthermore, promotes displacement of adsorbed DMMP by H_2O, at sufficiently high RH, in favor of the formation of the ice-like layer. The solubility limit of DMMP in H_2O is estimated[80] to be 4.95 M at 25 °C and pH 7. When this is exceeded, a layer of liquid-like DMMP (with ν(P=O) ≈ 1245 cm^{-1}) is expected to form. Some evidence for this might be seen in the asymmetry of the ν(P=O) peak in Figure 7d.

(80) Lu, X.; Nguyen, V.; Zeng, X.; Elliott, B. J.; Gin, D. L. *J. Membrane Sci.* **2008**, *318*, 397.

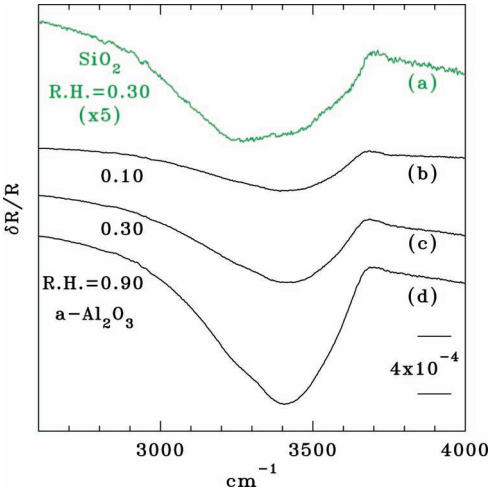

Figure 8. Similar to Figure 1 but showing data for a-Al_2O_3. Only a few selected RH values are shown. For comparison, (a) shows similar data for H_2O adsorption on thermal a-SiO_2 at RH = 0.30, multiplied by a factor of 5 relative to those for Al_2O_3. The different traces have been shifted vertically for clarity. Note the difference in the R/R scale vs Figure 1.

3.1.4. Thermal vs UV/O_3 Oxide. The data presented thus far were all obtained for a UV/O_3 oxide. All experiments were repeated for a thermal oxide, and the results were virtually identical to those given above. One small exception was in the growth of the H_2O layer (Figure 1). For the thermal oxide at low RH (< 0.30) the ν(O−H) spectrum was dominated by the ice-like band and closely resembled data for a UV/O_3 oxide given in ref 3. At higher RH, on the other hand, the ν(O−H) spectra for both types of oxide were essentially identical.

3.2. Amorphous Al_2O_3. Figures 8 and 9 show data for amorphous Al_2O_3 vs RH (in the absence of DMMP). The ν(O−H) spectrum shows only liquid-like H_2O with no evidence of an ice-like band at any RH in the range of 0.02 to 1.0. A weak shoulder near ~3250 cm^{-1}, seen at very high RH, can be assigned to the overtone of the 1640 cm^{-1} δ(HOH) mode (not shown). Figure 8a shows, for comparison, the spectrum for SiO_2 at RH = 0.30. In addition to the absence of an ice-like layer, a-Al_2O_3 shows a higher H_2O coverage than does SiO_2 at the same RH, as is evident in comparing the isotherms in Figures 2 and 9. Following these experiments, XPS showed no significant increase in the OH content (see the Supporting Information).

Figure 10 shows results for pure DMMP (in the absence of H_2O) and for the coadsorption of H_2O and DMMP. As in the case for H_2O, the DMMP coverage indicated by the IR band intensities is higher than on SiO_2 at the same P/P_0. Both observations are consistent with the higher coverage of OH groups on a-Al_2O_3 as seen in the O 1s XPS (see the Supporting Information) and with the importance of H-bonding to OH in the adsorption of both H_2O and DMMP. The trend in ν(P=O) with increasing P/P_0 is similar to that seen for SiO_2 in Figure 4. However, at very low P/P_0, ν(P=O) appears about 1226 cm^{-1}, which is somewhat lower than for SiO_2 and suggests a stronger O—H···O=P bond. Results obtained under vacuum conditions for DMMP adsorption on HSA Al_2O_3 are useful for comparison. Here bonding occurs via Al···O=P interaction at coordinatively unsaturated Al sites giving ν(P=O) at 1216 cm^{-1} (refs 44a and 46a), which is significantly red-shifted from the present results for Al—OH···O=P bonding. A further discussion of the a-Al_2O_3 results is given in the following section.

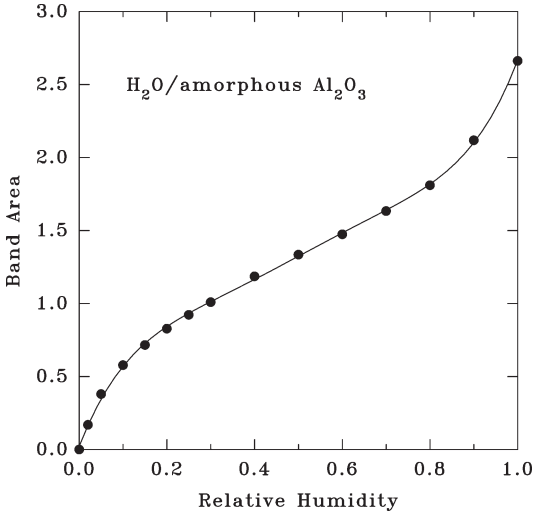

Figure 9. Similar to Figure 2 but showing data for Al_2O_3. Note the difference in the band area scale vs Figure 2.

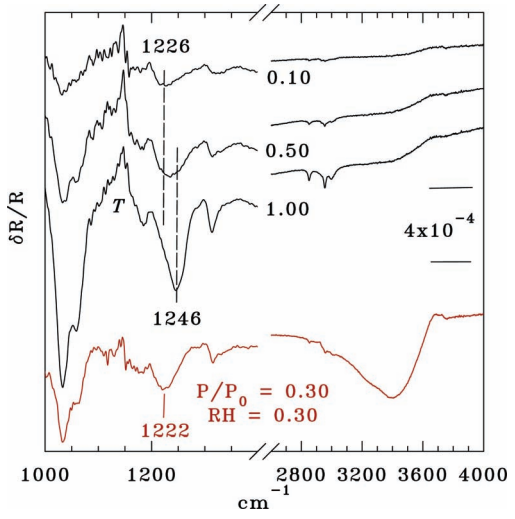

Figure 10. Similar to Figures 4 and 6 but showing results for DMMP on a-Al_2O_3. The numbers 0.10, etc. give the DMMP P/P_0 in the absence of intentionally added H_2O. The "***T***" marks a miscanceled Teflon absorption from the ATR cell. The bottom trace shows data for coadsorption of DMMP (P/P_0 = 0.30) and H_2O (RH = 0.30). The spectra have been displaced vertically for clarity, and the dashed lines show the position of the ν(P═O) mode, which changes with P/P_0. Note the difference between the $\delta R/R$ scales here and in Figures 4 and 6.

3.3. Highly-Hydroxylated a-Al_2O_3. It is known[81,82] that prolonged exposure of Al_2O_3 to liquid H_2O converts the surface to a mixture of AlO(OH) and $Al(OH)_3$, with the detailed chemistry depending on the method of treatment (e.g., on the H_2O temperature). A preliminary study was done of the effects of such "weathering" on the interaction with DMMP. To simulate one form of a highly hydroxylated Al_2O_3 surface, 4 nm of Al metal was vapor-deposited on each side of a Si ATR prism and each side subsequently exposed to UV/O_3 for one hour at nominal room temperature. (Radiative heating by the UV lamp raised the sample temperature to about 40 °C by the end of the exposure.)

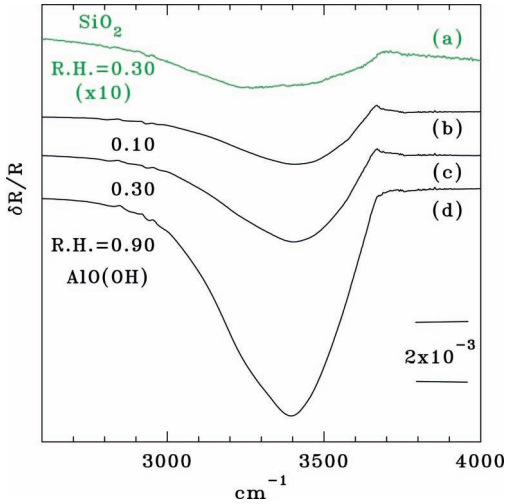

Figure 11. Similar to Figure 1 but showing ν(O−H) vs RH for H_2O/AlO(OH). Only a few selected RH values are shown. The spectrum for SiO_2 at RH = 0.30 is the same as that shown in Figure 8a and is included for comparison, multiplied by a factor of 10 relative to the AlO(OH) data.

This is known[83,84] to produce a high-quality a-Al_2O_3 film up to a limiting thickness of about 2 nm. The sample was then immersed in boiling DI H_2O for 15 min. Characterization of the resulting film using XPS and transmission IR data (see the Supporting Information) indicated the presence of Al oxyhydroxide, AlO(OH), in the so-called "pseudoboehmite" or "poorly-crystalline boehmite (PCB)" form with no metallic Al remaining.

There are many similarities between the results for PCB and those for a-Al_2O_3 discussed in the preceding section. The ν(OH) spectrum vs RH (Figure 11) shows only liquid H_2O with no obvious ice-like layer at any RH. This concurs with previous IR transmission results[85] for PCB in contact with H_2O vapor. The weak shoulder seen at ~3250 cm^{-1} at high RH has been assigned[85] to the overtone of the δ(H−O−H) bending mode at 1640 cm^{-1} (not shown). The integrated band area at any RH (Figure 12) is significantly greater than for either SiO_2 (Figure 2) or a-Al_2O_3 (Figure 9) at the same RH, and the isotherm is similar in shape to that reported earlier[85] for H_2O on PCB. These observations are consistent with a high density of OH groups (documented in the Supporting Information) that act as adsorption sites. The initial exposure of this surface to H_2O (Figure 11) results in an upward-pointing peak at 3660 cm^{-1} due to the removal, through adsorption, of free OH (i.e., groups not involved in H-bonding to each other or to H_2O). Very weak structure in the 2800−3000 cm^{-1} range arises from either miscancellation of features in the single-beam spectra due to organic contamination in the FTIR beamsplitter or to a small amount of impurity actually present on the sample.

Adsorbing DMMP on this surface (Figure 13) gives results similar to those discussed above. A strong O—H···O═P interaction occurs at low P/P_0, leading to a large red-shift in ν(P═O) relative to the vapor (1231 vs 1276 cm^{-1}), followed by the formation of liquid-like DMMP at higher P/P_0. At high P/P_0 a shoulder is seen on the high-energy side of the 1246 cm^{-1} liquid-like ν(P═O) peak, which is not evident in the case of adsorption on SiO_2 (Figure 4). This feature, which is also seen for a-Al_2O_3 (Figure 10), might indicate the formation of DMMP clusters

(81) Lefèvre, G.; Duc, M.; Lepeut, P.; Caplain, R.; Féderoff, M. *Langmuir* **2002**, *18*, 7530.
(82) Desset, S.; Spalla, O.; Lixon, P.; Cabane, B. *Colloid Surf. A* **2002**, *196*, 1.
(83) Popova, I.; Zhukov, V.; Yates, J. T., Jr. *Surf. Sci.* **2002**, *518*, 39.
(84) Chang, C.-L.; Engelhard, M. H.; Ramanathan, S. *Appl. Phys. Lett.* **2008**, *92*, 263103.
(85) Wang, S.-L.; Johnston, C. T.; Bish, D. L.; White, J. L.; Hem, S. L. *J. Colloid Interface Sci.* **2003**, *260*, 26.

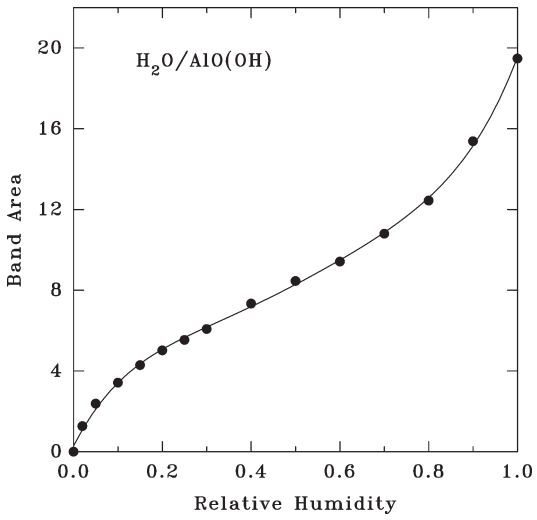

Figure 12. Similar to Figure 2 but showing results for H_2O/AlO(OH).

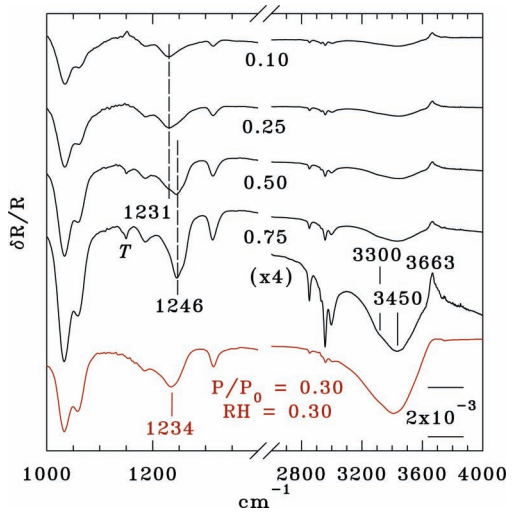

Figure 13. Similar to Figures 4 and 6 but showing results for DMMP on AlO(OH). The numbers 0.10, etc. give the DMMP P/P_0 in the absence of intentionally added H_2O. The "***T***" marks a miscanceled Teflon absorption from the ATR cell. The bottom trace shows data for coadsorption of DMMP (P/P_0 = 0.30) and H_2O (RH = 0.30). The spectra have been displaced vertically for clarity, and the dashed lines show the position of the ν(P═O) mode, which changes with P/P_0. Note the difference between the $\delta R/R$ scales here and in Figures 4 and 6. The high-energy end of the P/P_0 = 0.75 spectrum is also shown with a 4× vertical expansion.

rather than a homogeneous liquid. Molecules on the periphery of such clusters would be in an environment that is partly liquid- and partly vapor-like. As in the case of H_2O, the DMMP band intensities at a given P/P_0 are all significantly greater than for adsorption on SiO_2 (Figure 4) or on a-Al_2O_3 (Figure 10). Two ν(O−H) bands, for OH groups in OH···O═P bonds, are seen at about 3300 and 3450 cm^{-1}. These are tentatively assigned, respectively, to Al−OH groups strongly bound to DMMP and to Al−OH and/or H_2O weakly interacting with DMMP. As in the case of H_2O (Figure 11), a prominent upward-pointing peak is seen at 3663 cm^{-1} for the lowest P/P_0, which results from the removal of free OH groups. The intensity of this feature saturates at low P/P_0 indicating that such sites are energetically favored for adsorption.

A significant issue is the appearance, at low P/P_0, of ν(P═O) at about 1226 cm^{-1} for a-Al_2O_3 (Figure 10) vs 1231 cm^{-1} for AlO(OH) (Figure 13). It has previously been noted[48] that the adsorption energy of DMMP on hydroxylated γ-Al_2O_3 increases with the Bronsted acidity of the OH site. It has also been found[86] that OH sites on PCB AlO(OH) are less acidic than on other forms of Al oxide, which is consistent with the higher ν(P═O) frequency (i.e., less red-shifted from the gas phase) seen here for DMMP on PCB. This difference persists, and even increases, when DMMP and H_2O are coadsorbed. Here ν(P═O) appears at 1222 cm^{-1} for a-Al_2O_3 and at 1234 cm^{-1} for AlO(OH). This suggests that DMMP remains bonded to Al−OH in the presence of added H_2O rather than being displaced, i.e., "dissolved". If the DMMP were in an essentially aqueous environment, as is thought to be the case for coadsorption on SiO_2 (see section 3.1.3), one would expect ν(P═O) to fall at the same frequency for both a-Al_2O_3 and AlO(OH). This would presumably be ∼1226 cm^{-1}, which is the position observed for coadsorption on SiO_2. It must be noted, however, that although this model explains why ν(P═O) is different for the two surfaces it does not account for the fact that the difference increases when H_2O is added.

Following these experiments the Al_2O_3 and AlO(OH) samples were checked for residual phosphorus that would indicate partial decomposition of the DMMP. This has been reported[44−46] to occur on HSA Al_2O_3 powders at somewhat above room temperature. No P 2p XPS peak, with a binding energy of ∼130 eV, or P LMM X-ray-excited Auger emission, at a kinetic energy of ∼120 eV, was observed.

4. Summary

Infrared ATR spectroscopy has been applied to a study of the interaction of DMMP with amorphous SiO_2, Al_2O_3, and AlO(OH) surfaces as a function of RH. The results are as follows.

(1) For H_2O/SiO_2 the growth, with increasing RH, of an ice-like and a liquid-like layer has been seen here in agreement with previous work. The growth appears to depend on the surface condition but not directly on how the oxide is grown. Observation of H ↔ D exchange during exposure of the H_2O layer to D_2O indicates that the ice-like layer is more resistant to exchange, consistent with a stronger intermolecular interaction than in the liquid-like layer.

(2) H ↔ D exchange during exposure of an SiO_2 surface to D_2O, after purging with dry N_2 at room temperature, indicates the existence of a layer of adsorbed H_2O that, however, does not exhibit an ice-like IR spectrum. The ice-like layer appears only in an ambient with a finite RH and forms in addition to the preadsorbed H_2O, which might then function as a transition layer or be incorporated into the ice-like layer.

(3) Exposure of SiO_2 to DMMP vapor with increasing P/P_0, in the absence of intentionally added H_2O, shows the sequential formation of a strongly interacting molecular species followed by a liquid-like DMMP layer. The strong interaction involves SiO—H···O═P bonds to surface silanols and/or HO—H···O═P bonds to preadsorbed molecular H_2O.

(4) At a finite RH the ice-like layer forms on SiO_2 even in the presence of DMMP up to P/P_0 = 0.30. This is taken to indicate a mixture of liquid-phase H_2O and DMMP (essentially a two-dimensional solution) existing on top of an intact ice-like layer. DMMP

(86) van den Brand, J.; Snijders, P. C.; Sloof, W. G.; Terryn, H.; de Wit, J. H. S. *J. Phys. Chem. B* **2004**, *108*, 6017.

does not appear to penetrate the ice-like layer readily under these conditions, and the tendency to form a such a layer provides a driving force for displacing adsorbed DMMP.

(5) Amorphous Al_2O_3 and poorly crystalline (or pseudo-) boehmite (AlO(OH)) do not exhibit an ice-like H_2O layer at any RH in the range of 0.02 to 1.0. Both have a higher content of surface OH than does SiO_2, which leads to higher coverages of H_2O or DMMP at equivalent values of RH or P/P_0. At low P/P_0, for which adsorption is dominated by Al—OH···O=P bonding, *a*-Al_2O_3 interacts with DMMP more strongly than does AlO(OH). This results from the higher acidity of OH sites on *a*-Al_2O_3. In coadsorption, up to RH = 0.30 and P/P_0 = 0.30, DMMP appears to remain bonded to the surface rather than being displaced by H_2O.

(6) H_2O appears to have little or no effect on the total amount of DMMP adsorbed on any of the surfaces studied in this work, up to an RH of 0.30 and a DMMP P/P_0 of 0.30.

It is possible to suggest what implications these results might have regarding the transport and fate of DMMP and related molecules on oxide surfaces in the environment. At very low RH and low P/P_0, transport of DMMP across the surface of SiO_2 and similar materials will be kinetically limited by strong interactions with Si−OH groups and with surface-bound H_2O. At very low RH but higher P/P_0 a liquid-like DMMP layer forms on top of this strongly bound layer. In this case, the liquid-like DMMP "sees" not the bare surface but the layer of strongly bound H_2O and DMMP, which then controls the interaction with the substrate. With increasing RH, the stability of the ice-like H_2O layer promotes displacement of surface-bound DMMP. It is expected that DMMP will then become more mobile within the thin aqueous solution that forms on top of the ice-like layer. At high P/P_0, when the solubility limit of DMMP in H_2O is exceeded, it is expected that a layer of liquid-like DMMP will form on top of a layer of saturated aqueous solution.

On the other hand the Al oxide materials studied here do not exhibit an ice-like layer. The surface OH content and, in the case of *a*-Al_2O_3, the OH acidity are higher than for SiO_2. As a result, DMMP adsorbed on these surfaces is not displaced by H_2O, at least up to an RH of about 0.30. However, at high P/P_0, a liquid-like DMMP layer (which is presumably mobile) forms on top of the mixed layer of DMMP and H_2O strongly bound to Al−OH groups.

Further studies involving aqueous solutions of DMMP in contact with oxide surfaces are needed to extend the range of the present work to higher densities of H_2O and DMMP.

Acknowledgment. This work was funded and supported by contract TAS-CBS.FATE.03.10.NRL.001 from the Defense Threat Reduction Agency (DTRA). D. E. Tevault is thanked for several helpful communications. A. Snow is thanked for help with the contact angle measurements, D.Y. Petrovykh for help with the XPS measurements and E. E. Foos and K. D. Hobart for providing the UV/O_3 facilities. F. K. Perkins is thanked for growing the thermal SiO_2 film.

Supporting Information Available: Procedure for determining SiO_2 thickness using XPS; procedure for determining Al_2O_3 thickness using XPS; procedure for determining surface impurity levels using XPS; procedure for determining oxide-layer stoichiometry using XPS; surface analysis of SiO_2 using XPS; surface analysis of Al_2O_3 using XPS; surface analysis of hydroxylated Al_2O_3 using XPS; characterization of SiO_2 and Al_2O_3 films using IR transmission. This material is available free of charge via the Internet at http://pubs.acs.org.

Note Added in Proof. Very recently a paper has appeared[87] which reports a molecular dynamics study of the interaction of DMMP with SiO_2 surfaces in the presence of H_2O.

(87) Quenneville, J.; Taylor, R. S.; van Duin, A. C. T. *J. Phys. Chem. C* **2010**, *114*, 18894.